

# Centrality Dependence of Low Momentum Direct Photon Production in $\sqrt{s_{NN}} = 200\text{GeV}$ Au+Au Collisions in PHENIX

**R Petti**

Department of Physics and Astronomy, Stony Brook University, Stony Brook, NY 11794-3800, USA

E-mail: richard.petti@gmail.com

**Abstract.** Interest in the production of direct photons at low momentum in heavy ion collisions has increased recently with the rather puzzling recent PHENIX results on the observation of a large excess in the yield of direct photons in Au+Au collisions compared to the  $N_{coll}$  scaled p+p yield and the observation of a large direct photon  $v_2$  at  $p_T$  below  $3\text{GeV}/c$ . The two measurements are difficult to reconcile within the current understanding of the fireball evolution and the assumption that low momentum direct photons are dominantly emitted early in the collision. This has sparked much theoretical interest, with new calculations refining old works as well as calculations of newly proposed production mechanisms. Experimental constraints on newly proposed production mechanisms are crucial in understanding the evolution of the fireball. One would also desire experimental evidence whether the direct photons below  $p_T$  of  $3\text{GeV}/c$  are dominantly emitted early or late in the collision. In this proceedings, we show new PHENIX measurements of the detailed centrality dependence of direct photon production in the range of  $0.4 < p_T < 5\text{GeV}/c$  in Au+Au collisions at  $\sqrt{s_{NN}} = 200\text{GeV}$  based on the high statistics of the combined 2007 and 2010 datasets. Photons are cleanly identified through their external conversion in the backplane of the Hadron Blind Detector to dielectron pairs. We observe the shape of the excess direct photon invariant yield in the range of  $0.6 < p_T < 2\text{GeV}/c$  is well described by an exponential fit with an inverse slope of  $240\text{MeV}/c^2$ , consistent with previous measurements. Additionally, the shape is seen to be the same for all centralities within uncertainties and the integrated yield follows a power law as a function of  $N_{part}$ . The new results will offer powerful constraints to current calculations which must predict the same centrality dependence.

## 1. Introduction

Direct photons are an essential probe of heavy ion collisions. Because of their negligible interaction cross-section with the partonic medium, photons can escape the medium virtually unmodified, carrying with them information about the conditions of the system at the time of the photon's production. This allows experimental access to the entire space-time evolution of the system. The difficulty lies in the inability to experimentally separate various contributions to the direct photon yield since we measure a time-integrated snapshot of photons from all sources. Direct photons are defined as any photon not originating from a hadron decay. Theoretical calculations must account for the measured spectra. These theoretical calculations need to include the various production rates for each mechanism of direct photon production integrated over the space-time evolution of the system.



We focus on low momentum ( $p_T < 5\text{GeV}/c$ ) direct photons in this proceedings. These soft photons should be sensitive to the temperature [1] and the underlying dynamics of the collision through the yield and the observed azimuthal anisotropy of emission relative to the reaction plane quantified by  $v_2$  [2][3] ( $v_2$  is the second order coefficient in the Fourier decomposition of the azimuthal angle distribution [4]). These soft photons also allow us to experimentally probe possible effects from large background magnetic fields [5][6] or very early time production (possibly in the Glasma [7]). For these reasons, PHENIX has a suite of measurements dedicated to soft photon production in Au+Au collisions [8][9][10][11]. We report on the latest measurement in this proceedings. The new measurement takes advantage of the excellent electron identification capabilities of the PHENIX Ring Imaging Cherenkov (RICH) detector to measure real photons via their external conversion in material to di-electron pairs. This method virtually eliminates the miss-identified hadron background that plagues previous analyses which measure the photon energy deposition directly in the electromagnetic calorimeters [4]. This allows us to push the measurement to lower momentum than was previously possible. To further reduce systematic uncertainties, we measure the direct photon fraction  $R_\gamma = \gamma^{incl}/\gamma^{hadron}$ , or the ratio of the yield of inclusive photons to photons from hadron decays, as a double ratio, which explicitly cancels major sources of systematic uncertainty.

## 2. Experimental Setup

The direct photon measurement discussed here is measured using the PHENIX detector, which is located at the Relativistic Heavy Ion Collider (RHIC) at Brookhaven National Lab (BNL) in Upton, NY. The PHENIX central arms make up a two arm spectrometer, with each arm covering  $90^\circ$  and separated by  $90^\circ$  in azimuth and covering  $-0.35 < \eta < 0.35$  in pseudo-rapidity. The details of the detector and the various subsystems are explained elsewhere [12]. We only briefly mention the main detectors used in this particular measurement.

The Beam-Beam Counter (BBC) is the main detector system used to measure the global properties of the collision, such as centrality and z-vertex, and resides in the north and south muon arms located in forward and backward directions along the beamline. The BBC detector consists of arrays of quartz radiators attached to photo-multiplier tubes arranged around the beampipe and sit about 1.5 meters down the beamline in both the north and south direction ( $3.1 < |\eta| < 3.9$ ).

The main photon measurement is made using the PHENIX tracking system, the RICH detector, and the electromagnetic calorimeters. The Hadron Blind Detector (HBD) [13] was also installed in 2007, but is used only as a source of photon conversions in this analysis. The bulk of the photons that convert in the HBD occur in the backplane, where readout electronics are located ( $X/X_0 \approx 3\%$ ), which resides at a radius of about 60cm from the interaction point.

The PHENIX tracking system in each arm consists of drift chambers (DCH) and various layers of pad chambers (PC), which allow us to track particles through the magnetic field, give a measurement of momentum, and provide pointing to the other detector systems. The RICH detector is the main electron ID detector. Only electrons Cherenkov radiate in the  $Ar/CO_2$  gas mixture inside the detector up to about  $5\text{GeV}/c$ , where pions also start to radiate. We reconstruct the rings from the Cherenkov radiation of the electrons that are reflected onto arrays of photo-multiplier tubes residing outside of the experimental aperture. The electromagnetic calorimeters (EMCAL) are the outer most detector in the central arms of PHENIX. Here we measure the energy and direction of photons, as well as electrons which assists in the electron identification through the energy to momentum ratio.

## 3. Photon Identification

A novel approach in PHENIX is used to identify photons in this analysis. Hadron mis-identification is a major source of systematic uncertainty in analyses that measure photons

in the EMCAL directly. We avoid this issue in the current analysis by measuring photons that externally convert in the backplane of the HBD detector (radius  $\approx 60\text{cm}$ ). The novel approach utilizes the feature that far off-vertex particles will be reconstructed with a slightly wrong momentum, due to the fact that PHENIX does all of its tracking outside of the magnetic field, and so assumes that all particles originate from the event vertex in the track reconstruction. The effect is illustrated in Fig. 1. The figure shows a photon (white line) being emitted from the event vertex of the collision. The photon is shown to convert in the HBD and the  $e^+$  and  $e^-$  (indicated by the red lines) leave hits in the detector systems described in the previous section. If we take the hits left by the tracks and incorrectly trace them through the field to the event vertex (shown by the yellow lines), we see in the exaggerated cartoon that the pair obtains an artificial opening angle. This translates to an apparent mass for the pair. The magnitude of the mass is proportional to the radius of conversion.

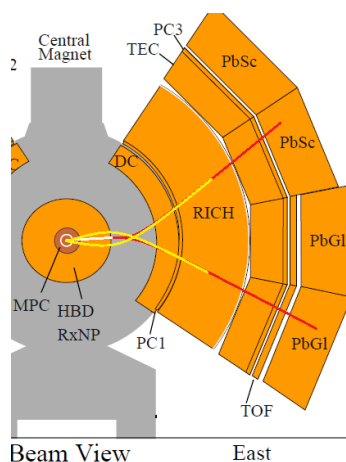


**Figure 1.** A cartoon illustrating the effect of the false assumption of the event vertex origin on a di-electron pair from a photon conversion in the backplane of the HBD, resulting in an artificial opening angle. The true track trajectory is shown in red, the (incorrect) traceback to the event vertex is shown by the yellow lines.

Detailed GEANT Monte Carlo simulations have been done to study the miss-reconstruction effect on conversion pairs. Conversions that occur at a radius of  $60\text{cm}$  obtain a pair mass of about  $12\text{MeV}/c$  in the field setting used in 2007 and 2010. We use the simulations to correct for the miss-reconstruction effect. To achieve this, we reparameterize the momenta of each track under an alternate track model assumption, that each track originated from  $60\text{cm}$  rather than from the event vertex. This gives us two masses for each pair. A view of the 2D mass distribution in the data is shown in Fig. 2. The vertical axis shows the pair invariant mass calculated under the alternate track model of the HBD backplane origin ( $M_{hbd}$ ). The horizontal axis shows the pair invariant mass calculated under the standard reconstruction assuming the event vertex origin ( $M_{vtx}$ ). A correlation can be seen between the two for HBD backplane conversions. The large peak sitting at  $M_{hbd} \approx 2\text{MeV}/c^2$  and  $M_{vtx} \approx 12\text{MeV}/c^2$  is due to the backplane conversions. The smaller peak observed to the left is due to Dalitz pairs from  $\pi^0$ s. These peaks sit on a low background due to combinatorial background. The contamination of our photon sample is estimated to be 1%. This method allows for a very clean separation of di-electron pairs from photon conversions in the backplane of the HBD from other sources of di-electron pairs, and additionally eliminates miss-identified hadron contamination. This powerful photon identification technique is essential to the measurement.

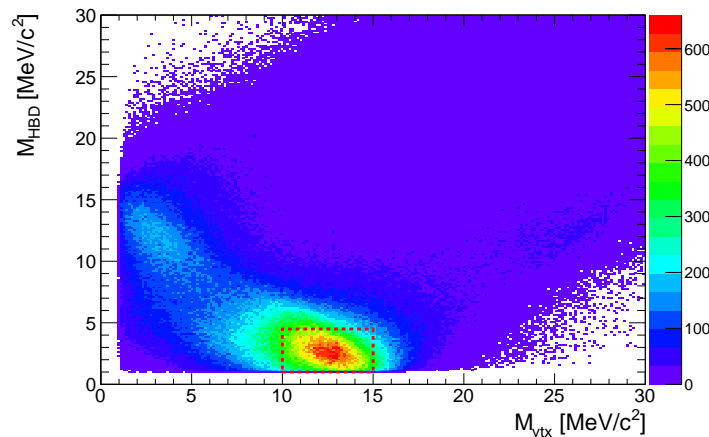


**Figure 2.** The distribution of di-electrons pairs in the  $M_{vtx}, M_{hbd}$  space. This is also the space which defines the cut that is used to isolate the photons (shown by the red box).

#### 4. Analysis

We start the analysis by quantifying the direct photon signal present through the direct photon fraction. The signal is quantified by the ratio  $R_\gamma = \gamma^{incl}/\gamma^{hadron}$ , or the ratio of the inclusive photon yield to the yield of photons coming from hadron decays. To reduce systematic uncertainties, we express  $R_\gamma$  as a double ratio, shown in Eqn. 1. The numerator of the double ratio consists of a ratio that is measured from the data, the ratio of the observed inclusive photon yield ( $N_\gamma^{incl}$ ) to the observed yield of inclusive photons that are tagged as coming from a  $\pi^0$  decay ( $N_\gamma^{\pi^0}$ ). A subset of the inclusive photons are tagged as coming from a  $\pi^0$  decay by pairing the converted photons with photons measured directly in the EMCAL to reconstruct the pions. Everything is performed and measured as a function of the converted photon  $p_T$ . This is important because when we form the ratio of the inclusive to pion tagged photon yield, the  $e^+e^-$  pair reconstruction efficiency and acceptance explicitly cancel, since these corrections are common factors to both the inclusive and pion tagged yields. Additionally, the probability of photon conversion also drops out. This significantly reduces the overall systematic uncertainty on the measurement and allows us to push down to very low  $p_T$ . The remaining corrections shown in Eqn. 1 concern the acceptance ( $f$ ) and reconstruction efficiency ( $\varepsilon_\gamma$ ) of getting the second leg of the pion decay into the EMCAL. The  $\langle \rangle$  around the correction indicates that we average over all EMCAL photon  $p_T$ , since we estimate the corrections as a function of the converted photon  $p_T$ . The largest source of systematic uncertainty (4%) concerns the  $\langle \varepsilon_\gamma f \rangle$  correction and the influence of the minimum  $p_T$  cut on the EMCAL photon of 600MeV (400MeV) for the 2007 (2010) analysis and the energy scale match in the simulation and the data. Details of the cuts and systematic uncertainties can be found in [11].

$$R_\gamma = \frac{\gamma^{incl}}{\gamma^{hadron}} = \frac{\langle \varepsilon_\gamma f \rangle \left( \frac{N_\gamma^{incl}}{N_\gamma^{\pi^0}} \right)_{data}}{\left( \frac{\gamma^{hadron}}{\gamma^{\pi^0}} \right)_{sim}} \quad (1)$$

The  $\pi^0$  reconstruction is shown for two example converted photon  $p_T$  bins in Fig. 3. As can be seen, the combinatorial background is successfully described and subtracted using a mixed event technique in which converted photons from one event are paired with EMCAL photons from completely different events within the same event class (characterized by z-vertex and

centrality).

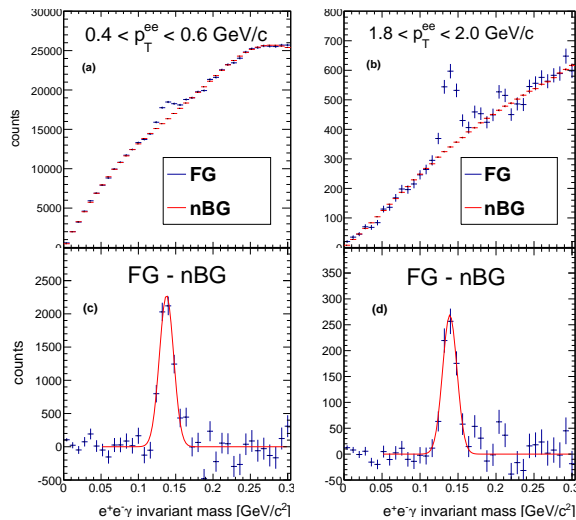


**Figure 3.** The  $\pi^0$  reconstruction illustrated in two  $p_T$  bins. Panels (a) and (b) show the converted photon-emcal photon pairs before combinatorial background subtraction, with the raw data (FG) in blue and the combinatorial background (nBG) in red. Panels (c) and (d) show the extracted  $\pi^0$  peak after background subtraction. The peak is fit with a Gaussian to estimate the peak position and width.

The  $\langle \varepsilon_\gamma f \rangle$  correction is calculated with two different implementations. The 2007 analysis calculates the correction with a full GEANT Monte Carlo simulation of  $\pi^0$  decays where one photon is forced to convert at 60cm. Occupancy effects on the reconstruction are taken into account by embedding simulated EMCAL hits into real data and reperforming the reconstruction. The 2010 analysis uses a “Fast Monte Carlo” approach, where effects from a full GEANT simulation are parameterized for faster event generation. The fast Monte Carlo was cross checked with the full Monte Carlo, the two were found to be consistent within uncertainties. The combined 2007+2010 result uses the fast Monte Carlo simulation for the correction on each dataset.

As described, we only measure the pion decay photon contribution to the inclusive yield directly. We estimate the remaining (sub-dominant) contribution from other hadrons in a hadron decay photon cocktail which includes  $\pi^0$ ,  $\eta$ ,  $\eta'$ , and  $\omega$  decays. We follow the same procedure as in [14]. The spectral shape of the pions is parameterized by fitting existing  $\pi^0$  data with a modified Hagedorn function. The shape of the remaining hadron species is then determined by  $m_T$  scaling, where the  $p_T$  in the Hagedorn function is replaced with  $m_T$ . The relative yields of each meson species is benchmarked to the pions and is taken from existing measurements. From the cocktail, we calculate the ratio of the yield of all decay photons to those just from  $\pi^0$  decays and insert into the denominator of Eqn. 1 to calculate  $R_\gamma$ .

As stated we combine the 2007 and 2010 results for a single  $R_\gamma$  measurement (after confirming that the individual results are consistent). From the high statistics  $R_\gamma$  measurement, we calculate the invariant yield of direct photons by scaling the hadron decay photon yield calculated in the same cocktail as described above appropriately by  $R_\gamma$  as shown in Eqn. 2. The results and a further analysis is shown in the next section.

$$\gamma^{direct} = (R_\gamma - 1)\gamma^{hadron} \quad (2)$$

## 5. Results

The combined 2007+2010  $R_\gamma$  measurement is shown in Fig. 4 for four different centrality bins. The previous measurement from the virtual photon analysis [9] is shown for comparison. The two results are consistent. As can be seen,  $R_\gamma$  is greater than one for each centrality, indicating a signal of direct photons in each centrality bin. Fig. 5 shows the invariant yield determined from the measured  $R_\gamma$  in the same centrality bins, shown by the points. Also included in the plots in each bin is the parameterized contribution of prompt processes, shown by the line. This parameterization is done by fitting a modified power law  $\left(a \left(1 + \frac{p_T^2}{b}\right)^c\right)$  to the direct photon yield measured in p+p collisions (which presumably only has prompt contributions) and then scaling by  $N_{part}$  for each corresponding centrality bin. An excess of direct photons above the scaled p+p yield is observed in all centralities.

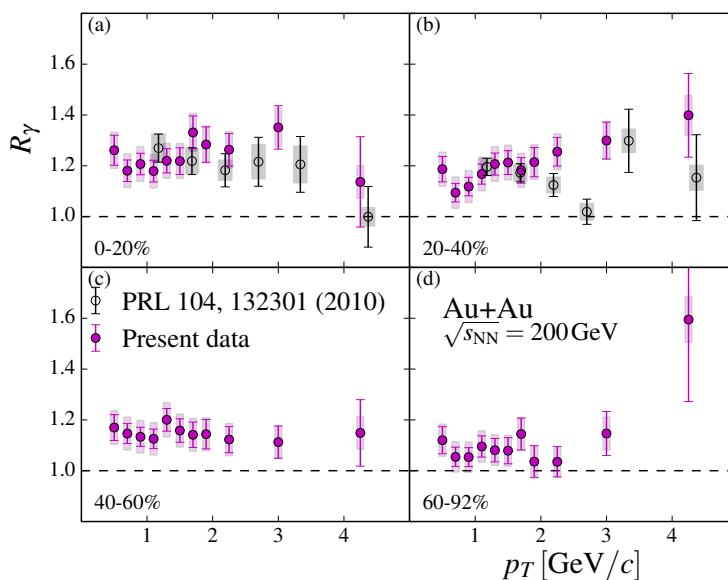


**Figure 4.** The measured  $R_\gamma$  shown for four centrality bins as indicated in the plots. This is the combined 2007+2010 analysis results.

We are not concerned with prompt contributions in this analysis; we want to focus on thermal radiation. Thus we subtract the scaled p+p yield shown by the line in Fig. 5 and display the observed excess yield in Fig. 6. We note that the entire spectrum cannot be described by a single exponential fit, although a large portion of it can (from 0.6-2.0 GeV/c). We perform the fit in this region and display the results in each panel of the figure. Note that within uncertainties, the extracted inverse slope from the fits are independent of centrality. We do a further analysis on the excess yield by looking at integrated yield as a function of  $N_{part}$ , as shown in Fig. 7. Since the first  $p_T$  point dominates a yield in these steeply falling spectra, we do the integration with different low  $p_T$  cutoffs, shown by the different colors in the figure. We observe that the shape of the excess yield as a function of  $N_{part}$  is the same at all  $p_T$  and can be described by a power law ( $A \cdot N^\alpha$ ) with a power  $\alpha = 1.48 \pm 0.08(stat) \pm 0.04(syst)$ .

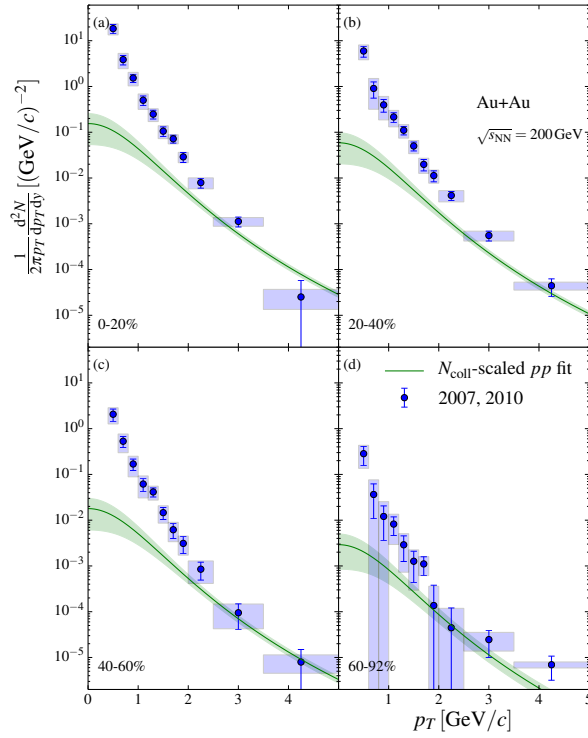


**Figure 5.** The direct photon invariant yield.

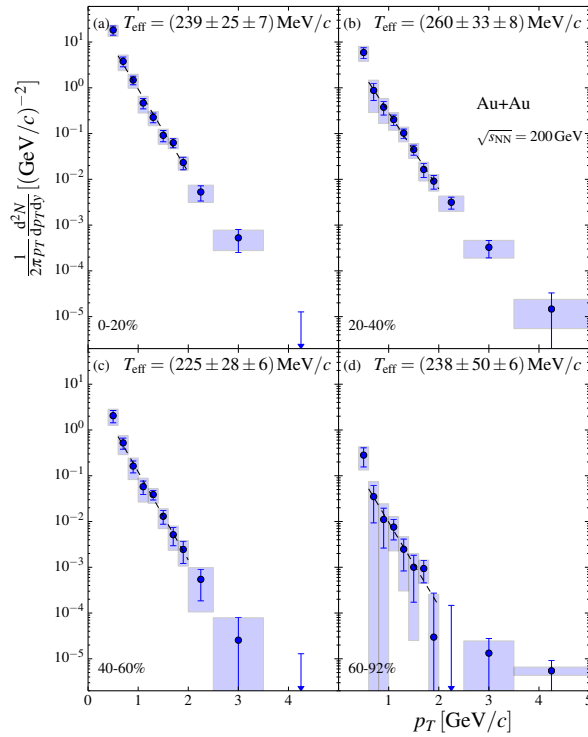


**Figure 6.** The isolated excess direct photon yield after scaled p+p contributions are subtracted.

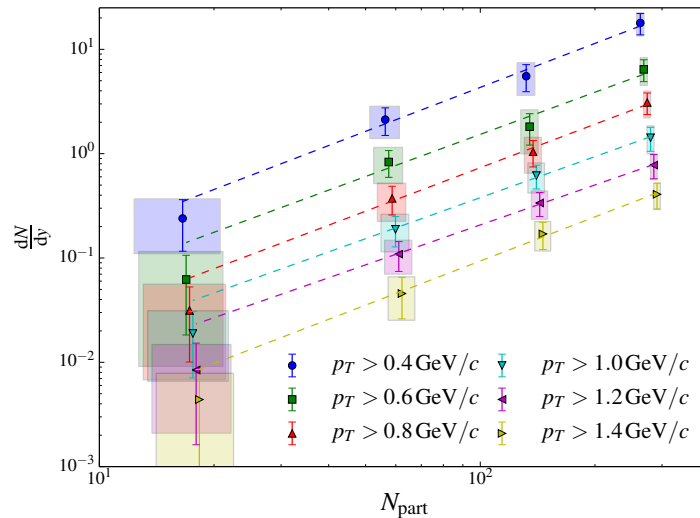


**Figure 7.** The integrated excess direct photon yield as a function of  $N_{part}$ . The different colors represent integrating with different low  $p_T$  thresholds.

## 6. Conclusions

We have discussed in this proceedings a new measurement from PHENIX of soft direct photon production in  $\sqrt{s_{NN}} = 200\text{GeV}$  Au+Au collisions at RHIC. We employ a novel photon identification procedure by measuring photons via their external conversion to di-electron pairs, taking full advantage of the excellent electron id capabilities of the PHENIX RICH detector. This virtually eliminates contamination from miss-identified hadrons. We also measure the direct photon fraction  $R_\gamma$  using a double ratio, which further reduces systematic uncertainties, allowing us to push the measurement all the way down to  $400\text{MeV}/c$  in  $p_T$ , a first in high energy heavy ion collisions. This allows us to explore the momentum region that is expected to be dominated by thermal radiation. We measure the direct photon invariant yield and isolate the excess production above the scaled p+p yield. We observe that the shape of the excess is independent of centrality and has a characteristic power law dependence as a function of  $N_{part}$ , with a power of  $\alpha = 1.48 \pm 0.08(stat) \pm 0.04(syst)$ . This measurement offers powerful constraints to theory calculations that claim to describe the evolution of the fireball produced in heavy ion collisions coupled with the direct photon production.

## References

- [1] Shen C, Heinz U W, Paquet J F and Gale C 2013 (*Preprint* 1308.2440)
- [2] Chatterjee, Srivastava, *Phys. Rev.* **C79**, 021901 (2009)
- [3] Linnyk O, Konchakovski V, Cassing W and Bratkovskaya E 2013 (*Preprint* 1304.7030)
- [4] Adare A *et al.* (PHENIX Collaboration) 2012 *Phys.Rev.Lett.* **109** 122302 (*Preprint* 1105.4126)
- [5] Tuchin K 2013 *Phys.Rev.* **C87** 024912 (*Preprint* 1206.0485)
- [6] Basar, Gokce, Kharzeev and Skokov 2012 *Phys.Rev.Lett.* **109** 202303 (*Preprint* 1206.1334)
- [7] Chiu M, Hemmick T K, Khachatryan V, Leonidov A, Liao J *et al.* 2013 *Nucl.Phys.* **A900** 16–37 (*Preprint* 1202.3679)
- [8] Adler S *et al.* (PHENIX Collaboration) 2005 *Phys.Rev.Lett.* **94** 232301 (*Preprint* nucl-ex/0503003)
- [9] Adare A *et al.* (PHENIX Collaboration) 2010 *Phys.Rev.Lett.* **104** 132301 (*Preprint* 0804.4168)
- [10] Afanasiev S *et al.* (PHENIX Collaboration) 2012 *Phys.Rev.Lett.* **109** 152302 (*Preprint* 1205.5759)
- [11] Adare A *et al.* (PHENIX Collaboration) 2014 (*Preprint* 1405.3940)
- [12] Adcox K *et al.* (PHENIX Collaboration) 2003 *Nucl. Instrum. Methods* **A499** 469
- [13] Anderson W *et al.* (PHENIX Collaboration) 2011 *Nucl. Instrum. Methods* **A646** 35
- [14] Adare A *et al.* (PHENIX Collaboration) 2010 *Phys.Rev.* **C81** 034911 (*Preprint* 0912.0244)